Vibration of a liquid-filled capillary tube

Shaobao Liu [a,b,c,1], Yufei Wu [c,d,1], Fan Yang [a], Moxiao Li [c,d], Xing Kou [d], Changsheng Lei [d], Feng Xu [b,c,**], Tian Jian Lu [a,d,*]

[a] State Key Laboratory of Mechanics and Control of Mechanical Structures, Nanjing University of Aeronautics and Astronautics, Nanjing, 210016, PR China
[b] The Key Laboratory of Biomedical Information Engineering of Ministry of Education, School of Life Science and Technology, Xi'an Jiaotong University, Shaanxi, 710049, PR China
[c] Bioinspired Engineering & Biomechanics Center (BEBC), Xi'an Jiaotong University, Xi'an, 710049, PR China
[d] State Key Laboratory for Strength and Vibration of Mechanical Structures, School of Aerospace, Xi'an Jiaotong University, Xi'an, 710049, PR China

ARTICLE INFO

ABSTRACT

Liquid-filled capillary tubes are common structures in nature and engineering fields, which often function via vibration. Although liquid-solid interfacial tension plays important roles in the vibration behavior of the liquid-filled capillary tube, it remains elusive how the interfacial tension influences the natural frequency of capillary tube vibration. To address this, we developed a theory of beam-string structure to analyze the influence of liquid-solid interfacial tension on the vibration of a liquid-filled capillary cantilever. We used glass capillary tubes as a demo and experimentally validated the theory, where the reduced liquid-solid interfacial tension in a capillary tube decreases the natural frequencies of small-order modes. We then performed theoretical analysis and found that the change of elastocapillarity number, slenderness ratio and inner/outer radius ratio of capillary tubes enables: in higher order modes, a nonmonotonic change of natural frequency due to mode transformation between a beam and string; for lower order modes, decrease in the natural frequency to zero (increase from zero) due to mode disappearance (appearance). The developed theory would provide guidelines for high-accuracy design of capillary sensors.

1. Introduction

Capillary tubes filled with different liquids and of different sizes are commonly found in nature (*e.g.* trichome (Liu et al., 2017; Zhou et al., 2017)) and engineering (*e.g.* microchannel resonator in MEMS (Belardinelli et al., 2017; Burg and Manalis, 2003)). The vibration of liquid-filled capillary structures plays significant roles in some of their functions and applications. For instance, the *Arabidopsis thaliana* leaf trichome is a complex liquid-filled capillary structure with branches, playing the roles of an active mechanosensory switch (Zhou et al., 2017) and acoustic antennae (Liu et al., 2017) through vibration. The suspended microchannel resonators are often used to characterize the mass, size of particles and cells in fluid (Bryan et al., 2013; Burg and Manalis, 2003; Godin et al., 2007). Microchannel resonators are also used to characterize the density (Kim et al., 2012; Najmzadeh et al., 2007) and

viscosity (Khan et al., 2013; Lee et al., 2012) of fluid based on the vibrational properties of the device. Therefore, it is of great importance to understand the vibration behaviors of liquid-filled capillary structures for the application of capillary sensors.

When the characteristic size of a structure decreases to microns or nanometers, the role of surface/interface tension becomes increasingly obvious in its mechanical behavior due to the increasing ratio of surface/interface area and volume (Sharma et al., 2003; Wang and Feng, 2007; Xia et al., 2011). For a microscale structure (*i.e.*, capillary tube), the role of liquid-solid interfacial tension on its vibration cannot be neglected. Some theoretical studies have been performed focusing on the vibration of beams (Marur and Prathap, 2005; Nandwana and Maiti, 1997) and liquid-filled pipes (no interfacial effect accounted for) (Gonçalves and Batista, 1988; Hatfield et al., 1982; Ting and Hosseini-pour, 1983). Numerical simulations based on finite element method

---

(FEM) have also been used to analyze the harmonic response and amplitude of capillary tubes without considering the interfacial effect (Gao et al., 2008; Hu et al., 1999). The effect of liquid-solid interfacial tension on the natural frequency of capillary tube vibration has not been thoroughly explored yet.

In this study, we developed a general theoretical model to understand the effect of liquid-solid interfacial tension on the natural frequency of a capillary tube. To verify the theory, we used glass capillary tubes as a demo and experimentally recorded the vibration of cantilever capillary tubes filled with solutions containing different concentrations of cleanser. The liquid-solid interfacial tension can be tuned by changing the concentrations of the cleanser and the effects of liquid-solid interfacial tension on vibration can be measured with a laser displacement sensor. With this validated model, we investigated the change of natural frequency with elastocapillarity number (dimensionless interfacial tension), slenderness ratio and inner/outer radius ratio of the capillary tube. The developed theory would provide guidelines for design of capillary sensors.

2. Theoretical analysis

2.1. Vibration theory of a liquid-filled capillary tube

Due to liquid-glass interfacial tension, the capillary tube may be regarded as the superposition of a cantilever beam and a string (*i.e.* beam-string structure). Fig. 1a shows the cross-section of the capillary and a micro-segment of the capillary with interfacial tension (γ_{sl}). Based on the vibration theories of Euler-Bernoulli beam (Timoshenko, 1983) and string (Carrier, 1945; Keller, 1959), the deflection of the capillary tube (u) is governed by:

$$-a^2\frac{\partial^4 u}{\partial x^4} + b^2\frac{\partial^2 u}{\partial x^2} = \frac{\partial^2 u}{\partial t^2} \tag{1}$$

where $a = \sqrt{\frac{EI}{\rho A}}$ and $b = \sqrt{\frac{T}{\rho A}}$; $T = 2\pi r_i \gamma_{sl}$ is the "string tension"; EI is the flexural rigidity of capillary tube; E is the Young's modulus and $I =$
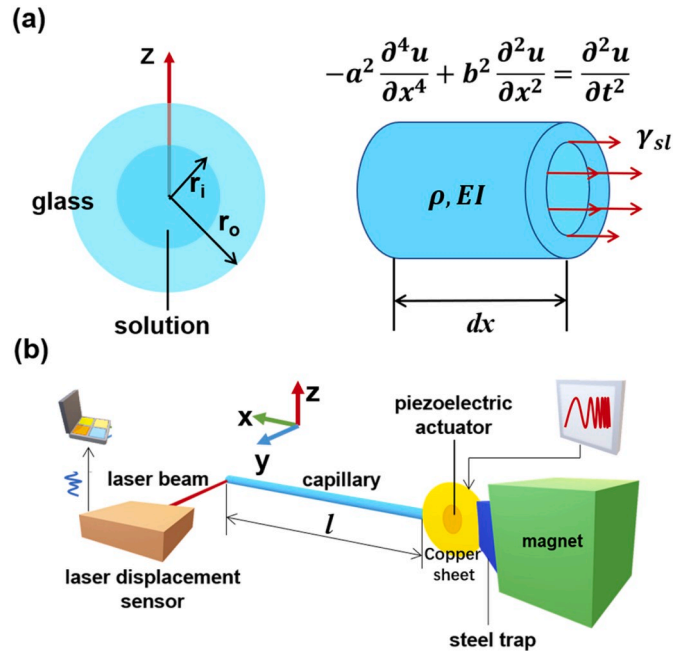

(a)

$$-a^2\frac{\partial^4 u}{\partial x^4} + b^2\frac{\partial^2 u}{\partial x^2} = \frac{\partial^2 u}{\partial t^2}$$

(b)

Fig. 1. (Color online) (a) A section and micro segment of a capillary tube with interfacial tension (γ_{sl}); (b) Experimental setting-up. Capillary tube is fixed on a piezoelectric patch clamped by a steel trap, which is fixed on a magnet base. Laser displacement sensor is used to detect the *y*-displacement at the free end of the capillary tube.

$\frac{\pi}{4}(r_o^4 - r_i^4)$ is the moment of inertia, in which r_i and r_o are inner and outer radius of the tube; $\rho = \rho_{solid} + \frac{A_{liquid}}{A_{solid}}\rho_{liquid}$ is the effective density of liquid-filled capillary tube; ρ_{solid} and ρ_{liquid} are the density of the tube and liquid in it, respectively. $A = \pi(r_o^2 - r_i^2)$ is the cross-sectional area of capillary tube, in fact $A = A_{solid}$; A_{liquid} is the cross-sectional area of the solution; γ_{sl} is the interfacial tension between the tube and liquid.

We consider that the capillary tube is fixed on one end and free on the other end, as:

$$\begin{cases} u(0,t) = 0, \frac{\partial u}{\partial x}\big|_{x=0} = 0, \frac{\partial^2 u}{\partial x^2}\big|_{x=l} = 0, \left(EI\frac{\partial^3 u}{\partial x^3} + T\frac{\partial u}{\partial x}\right)\big|_{x=l} = 0 \\ u\big|_{t=0} = 0, u_t\big|_{t=0} = 0 \end{cases} \tag{2}$$

where l is the length of capillary tube. Solving Eq. (1) with the method of variables separation and the boundary conditions of Eq. (2), we can obtain the following eigen equation of capillary tube vibration:

$$\begin{vmatrix} 0 & 1 & 0 & 1 \\ \alpha & 0 & \beta & 0 \\ 0 & 0 & A_{33} & A_{34} \\ A_{41} & A_{42} & A_{43} & A_{44} \end{vmatrix} = 0 \tag{3}$$

where $A_{33} = \beta[\alpha \sin(\alpha l) + \beta sh(\beta l)]$; $A_{34} = \alpha^2 cos(\alpha l) + \beta^2 ch(\beta l)$; $A_{41} = -EI\alpha^3 cos(\alpha l) + T\alpha cos(\alpha l)$; $A_{42} = EI\alpha^3 sin(\alpha l) - T\alpha sin(\alpha l)$; $A_{43} = EI\beta^3 ch(\beta l) + T\beta ch(\beta l)$; $A_{44} = EI\beta^3 sh(\beta l) + T\beta sh(\beta l)$. α and β are functions of angular frequency ω, as:

$$\begin{cases} \alpha = \sqrt{\dfrac{\sqrt{b^4 + 4a^2\omega^2} - b^2}{2a^2}} \\ \beta = \sqrt{\dfrac{\sqrt{b^4 + 4a^2\omega^2} + b^2}{2a^2}} \end{cases} \tag{4}$$

Upon substituting Eq. (4) into Eq. (3), the angular frequency of capillary tube ω can be solved with a numerical method. The dimensionless frequency (ω/ω_o) can be expressed using the dimensionless parameters of slenderness ratio (l/r_o), inner/outer radius ratio (r_i/r_o) and elastocapillarity number (γ_{sl}/Er_o) (see Supplementary Materials for the details). Here, the scaled frequency $\omega_o = \frac{1}{R}\sqrt{\frac{E}{\rho}}$ denotes the natural frequency of a solid beam with unit slenderness ratio but without interfacial tension (see Supplementary Materials for the details). The slenderness ratio, the inner/outer radius ratio and the elastocapillarity number can reflect the size effect of the capillary tube.

2.2. Frequency ratio of a beam to a string (FRBS)

Based on the analysis above, the capillary tube can be considered as a complex structure of beam and string. Thus, there are two extreme situations: pure beam and pure string. Based on classical vibration theories (Carrier, 1945; Keller, 1959; Timoshenko, 1983), the natural frequencies of a cantilever Euler-Bernoulli beam are given by:

$$w_{beam} = \beta_i^2\sqrt{\frac{EI}{\rho A}} \tag{5}$$

The boundary condition is

$$u(0,t) = 0, \frac{\partial u}{\partial x}\big|_{x=0} = 0, \frac{\partial^2 u}{\partial x^2}\big|_{x=l} = 0, \left(EI\frac{\partial^3 u}{\partial x^3}\right)\big|_{x=l} = 0$$

where $\beta_i l = \{1.8751, 4.6941, 7.8548, 10.9955, 14.1372, ...\}$ are the roots of $cos(\beta_i l)ch(\beta_i l) = -1$.

The natural frequencies of a one-end fixed string are:

$$w_{string} = \frac{(2i+1)\pi}{2l}\sqrt{\frac{2\pi r_i \gamma_{sl}}{\rho A}} \tag{6}$$

And the boundary condition is: $u(0,t) = 0, \left(\frac{\partial u}{\partial x}\right)|_{x=l} = 0$.

We defined the frequency ratio of a beam to a string (FRBS), as:

$$\phi = \frac{w_{beam}}{w_{string}} = \frac{2lr_o\beta_i^2}{(2i+1)\pi}\sqrt{\frac{(1-\eta^4)}{\eta\lambda}} \qquad (7)$$

where $\eta = r_i/r_o$, $\lambda = \gamma_{sl}/Er_o$. Note that ϕ is also proportional to a/b, reflecting the relative roles of the beam and the string in capillary tube vibration. The vibration of capillary tube is more like that of a string when ϕ is near zero. In contrary, the vibration of capillary tube is more like that of a beam when ϕ is much larger than 1. For a simply supported beam, Eq. (7) becomes: $\phi = \frac{i\pi r_o}{l}\sqrt{\frac{(1-\eta^4)}{\eta\lambda}}$.

3. Experimental methods

3.1. Experimental set-up for vibration measurement of liquid-filled capillary tube

We used a liquid-filled cantilever capillary tube to characterize the vibration behavior (Fig. 1b). We used two types of capillary tubes. Capillary tube I has a length of 100 mm and inner and outer diameters of 0.58 mm and 1 mm, respectively. Capillary tube II has a length of 100 mm and inside and outer diameters of 0.86 mm and 1.5 mm, respectively. We used glass tubes as an experimental demo to study capillary structures because the properties of glass are well known and it is convenient for experimental design of variables control. The y-direction displacement of the end of each capillary tube was detected using a laser displacement sensor (Micro-Epsilon, ILD2300), in which the laser power is less than 1mW. The chirp signal was used to drive tube vibration, which contains a large range of mode frequencies. In the experiment, we used the chirp signal with the frequency range of 20–1000 Hz (i.e., sweeping from 20 Hz to 1000 Hz), which can easily detect the natural frequencies in this range. Since each experiment with a certain interfacial tension took 30s, the heating effect of the laser on the liquid is negligible (increase of temperature less than 0.1 °C) and thus has little influence on the interfacial tension and density of liquid. One end of the capillary tube was attached to a piezoelectric patch driver and the other end is free. The piezoelectric patch is clamped on a steel trap that was attached to a magnetic base. In order to prevent the liquid in the tube from evaporating or flowing out, we used a layer of wax to fill both end of the tube. To verify the measurement approaches, we compared the spectrum map from experiment and simulation of an empty capillary tube (Fig. S4). The frequencies corresponding to the peaks in the spectrum map of simulation agree well with the experimental results, suggesting the present experimental approaches could well characterize the vibration behavior of capillary tubes.

3.2. Solution preparation

To explore the effect of interfacial tension (between glass and water) on the vibration of liquid-filled capillary tubes, a series of solutions with different surface tensions are needed. Cleanser (lower surfactant concentration) is commonly adopted to prepare solutions with proper concentrations, which is easily accessible and has little effect on other properties except surface tension. We thus prepared a series of water-based solutions with different volume fractions of cleanser (surfactants, water solvent, softening water and so on): 0, 0.1%, 0.2%, 0.3%, 0.4%, 0.5%, 0.8%, 1%.

3.3. Contact angle measurement

Measurement of contact angle is a common method to characterize the surface energy of a solution. We used glass slides (similar material and surface toughness with the capillary tubes) to measure the contact angle of liquid drops. We pipetted 1 μL of the prepared solutions onto the glass slide. Then, under an ultra-depth of field microscope (Keyence, VHX-5000), we took side-view pictures of the drop and measured the contact angles for solutions having different volume fractions of cleanser (Fig. S2a).

The surface tension of pure water at 25 °C is 71.96 mN/m (Vargaftik et al., 1983). According to the Young-Laplace equation ($\gamma_s = \gamma_l cos\theta + \gamma_{sl}$) and the Young-Good-Girifalco equation ($\gamma_{sl} = \gamma_s + \gamma_l - 2\sqrt{\gamma_s\gamma_l}$) (Girifalco and Good, 1957; Good and Girifalco, 1960), the surface tension (γ_l) and solid-liquid interfacial tension (γ_{sl}) can be calculated (Fig. S1, S2b&c, where γ_s is the surface tension of glass. When increasing volume fraction of cleanser, both γ_l and γ_{sl} decrease, approaching eventually a constant value. Fig. S2b&c show that in the range of 0–0.4%, surface tension and interfacial tension change obviously. Based on these results, the solutions with 0–0.4% cleanser were used for the present experiments.

4. Results and discussion

4.1. Validation of the theory

To study the effect of interfacial tension on the transverse vibration (y-direction) of the cantilever capillary tube, we used solutions with varying volume fractions of cleanser: 0, 0.1%, 0.2%, 0.3% and 0.4%, so that both the surface and interfacial tension display obvious changes. We used fast Fourier transform (FFT) to analyze the transverse vibration of the capillary tube in frequency domain.

As the volume fraction of cleanser is changed, the spectrum maps of liquid-filled capillary in transverse vibration show similar changes: the frequencies of peaks decrease with increasing cleanser volume fraction (Fig. 2a&b). That is because reducing the interfacial tension causes the natural frequency of each mode to decrease. Comparing the liquid-filled capillary tubes I and II in transverse vibration, we find that the spectrum map of capillary II (with smaller inside diameter) changes more obviously. We also found that when increasing the volume fraction of cleanser in solutions, the frequency of peak 2 changes little in capillary tube I (insert in Fig. 2a), but decreases more obviously within several Hertz in capillary tube II (insert in Fig. 2b). This result suggests the effect of interfacial tension on capillary vibration is size-dependent.

To verify the theoretical model, we compared the spectrum maps (Fig. 2a&b) between theory and experiment. The natural frequencies in theory and experiment agree well with each other (Fig. 2c). In theory, the effective Young's modulus is $E_{eff} = 1$ GPa, which is smaller than that of glass due to non-ideal fixed support (the cooper sheet is far from rigid). Except some modes that are not captured in measurement, the spectrum maps of the vibration in y direction agree well with the estimated results (Fig. 2a&b). The modes that are not captured in this direction can be detected in other directions. For instance, for tube II, the 1st and 4th order mode can be captured in z direction (Fig. S5). The measured natural frequencies of tube II agree well with the theoretical results (Fig. 2c), in which the 1st and 4th order modes are detected in z direction, while others are in y direction.

4.2. Influence of slenderness ratio

The dimensionless natural frequency (ω/ω_o) of the liquid-filled capillary tube decreases with slenderness ratio (l/r_o) and tends to zero when the slenderness ratio gets larger (Fig. 3a). Larger slenderness ratio means larger length or smaller radius (e.g., tends to zero) of the capillary tube. For the complex beam-string structure, larger length leads to smaller natural frequency of both the beam and string (Eqs. (5) and (6)). When the outer radius of the tube tends to zero, based on Eq. (1), $a{\to}0$ and $b{\to}\infty$, and hence the solution of (1) is in the form $u(x,t) = (px + q)\phi(t)$. Thus, the natural frequency tends to zero. That is, the natural frequency of liquid-filled capillary tube vibration decreases and tends to zero when the tube becomes slender.
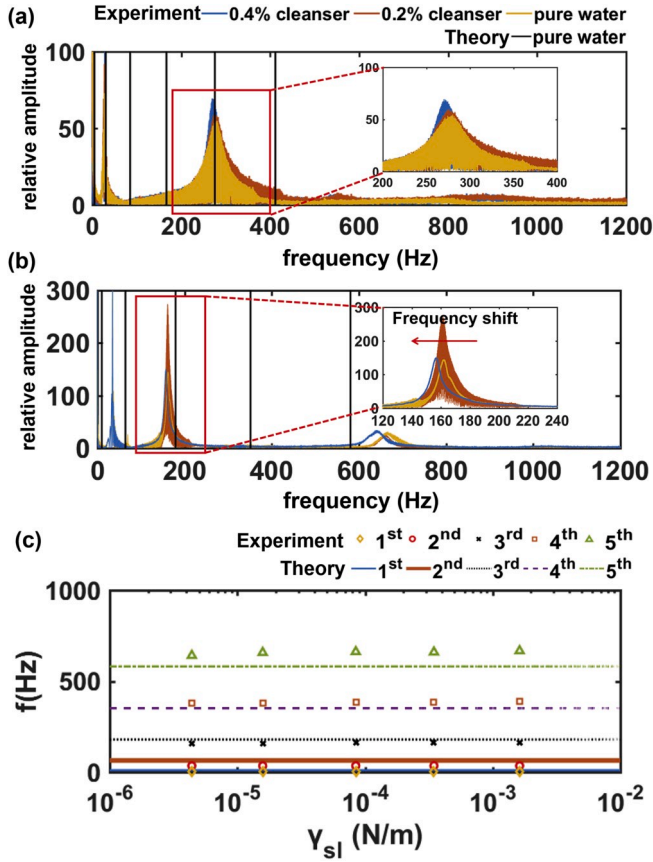
Fig. 2. (Color online) Comparison of spectrum map of capillary tube I (a) and II (b) between theory and experiment. (a) Frequencies of peak 1 and 2 are ~30 Hz and 270 Hz. (b) Frequencies of peak 1, 2 and 3 are ~30 Hz, 160 Hz and 650 Hz. (c) Comparison of natural frequency of capillary tube II between theory and experiment. The effective Young's modulus $E_{eff} = 1$ GPa. The 1st and 4th modes are detected in z direction experimentally, while other modes are detected in y direction.

4.3. Influence of elastocapillarity number

For the first-order mode of vibration, the dimensionless natural frequency decreases with increasing elastocapillarity number and finally disappears at a certain elastocapillarity number $(\gamma_{sl}/Er_o \sim 10^{-5})$ (Fig. 3b). That is because the capillary tube vibrates more like a string when elastocapillarity number is large. For a one-end fixed string, the energy/amplitude of low frequency decreases with the increase of characteristic parameter b $(= \sqrt{\frac{T}{\rho A}})$, which is positively correlated with elastocapillarity number. Thus, the mode with low frequency disappears when the elastocapillarity number is large enough.

For the second-order mode of vibration, with the increase of interfacial tension (S 5.1) or the decrease of Young's modulus (S 5.2)/outer radius (S 5.3), the dimensionless natural frequency firstly decreases and then increases, which is attributed to mode transformation: when the interfacial tension is small or the Young's modulus/outer radius is large ($\phi \gg 1$), the capillary tube mainly vibrates with the mode of a beam; in contrast, when increasing the interfacial tension or decreasing the Young's modulus/outer radius ($\phi \rightarrow 0$), the capillary tube mainly vibrates with the mode of a string. Except for the first two modes, with the increase of elastocapillarity number, the dimensionless natural frequencies increase (Fig. 3b). For higher modes, nonmonotonous variation of normalized natural frequencies does not occur in the present range of elastocapillarity number, for mode transformation needs larger elastocapillarity number for the higher order modes.
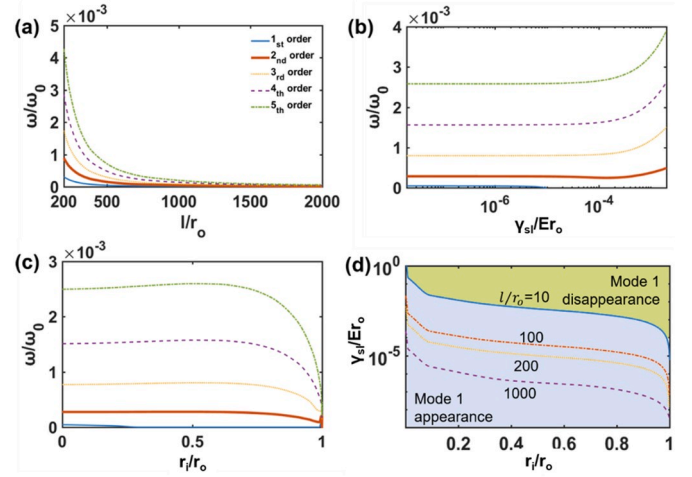

Fig. 3. (Color online) Effect of (a) slenderness ratio (l/r_o), (b) elastocapillarity number (γ_{sl}/Er_o) and (c) inner/outer radius ratio (r_i/r_o) on the dimensionless natural frequencies (ω/ω_o) of liquid-filled capillary tube vibration. (a) $r_i/r_o = 0.58$, $\gamma_{sl}/Er_o = 2 \times 10^{-5}$; (b) $r_i/r_o = 0.58$, $l/r_o = 200$; (c) $l/r_o = 200$, $\gamma_{sl}/Er_o = 2 \times 10^{-5}$. (d) Phase diagram of mode 1 with elastocapillarity number (λ) *vs.* inner/outer radius ratio (r_i/r_o).

4.4. Influence of inner/outer radius ratio

Except for the first-order mode, as the inner/outer radius ratio (r_i/r_o) of a capillary tube is increased to near unity, the natural frequencies first decrease and then increase to certain values of the natural frequency of an equivalent string having the same length and tension (Fig. 3c). That is because mode transformation from beam to string appears when the inner/outer radius ratio is near 1 ($\phi \rightarrow 0$). In the other range of the inner/outer radius ratio, the natural frequency first increases from the natural frequency of a beam of capillary tube without interfacial tension and then slightly decreases, because the natural frequency of the beam first increases and then decreases. For the first-order mode, the normalized natural frequency disappears at a certain inner/outer radius ratio ($r_i/r_o \sim 0.25$; Fig. 3c). That is because the capillary tube vibrates more like a string when the inner/outer radius ratio is large. For a one-end fixed string, the energy/amplitude of low frequency decreases with the increase of characteristic parameter b $(= \sqrt{\frac{T}{\rho A}})$, which is positively correlated with inner/outer radius ratio. Thus, the mode with low frequency disappears when the inner/outer radius ratio is large enough.

We presented the phase diagram of mode 1 with elastocapillarity number (γ_{sl}/Er_o) **vs.** inner/outer radius ratio (r_i/r_o) (Fig. 3d). With large elastocapillarity number and inner/outer radius ratio, mode 1 disappears. With the increase of slenderness ratio (l/r_o), the phase boundary shifts down, namely, there is more space of mode 1 disappearance. The phase boundary can be fitted as $\left(\frac{\gamma_{sl}}{Er_o}\right)\left(\frac{r_i}{r_o}\right)\left(\frac{l}{r_o}\right)^2 = 0.2161$.

In reality, when the first-order mode disappears, the natural frequency for each-order mode will be replaced by that of one-order-higher mode. Practically, the natural frequency for each-order mode will jump up. In contrary, when a new mode appears, the natural frequency for each-order mode will be replaced by that of one-order-lower mode, and the natural frequency for each-order mode will jump down.

5. Conclusion

We experimentally and theoretically studied the vibration behaviors of a liquid-filled capillary tube. We experimentally found that reducing the interfacial tension of the filling liquid decreases the natural frequencies of small-order modes. A theory of beam-string structure was developed to analyze the effects of elastocapillarity number, slenderness

ratio and inner/outer radius ratio on the vibration of the liquid-filled capillary cantilever beam. We introduced the frequency ratio of a beam to a string to understand the mode transformation between a beam and string. It was found that for higher order modes, nonmonotonic change of natural frequency is caused by mode transformation between the beam and the string; for lower order modes, the natural frequency decreases to zero (increases from zero) is attributed to mode disappearance (appearance). The study provides a framework to comprehend the vibration behaviors of capillary-elastic structures and guidelines for high-accuracy capillary sensors, such as microchannel resonators.

Although the properties of glass and cleanser are different from most of natural and engineering materials (*e.g.*, surface tension coefficient, Young modulus, density), in the proposed theory, the parameters and characteristic equation of natural frequency are in dimensionless form, which can be generalized to capillary-tube-like structures with different kinds of fluids such as biological capillary tubes (*e.g.*, trichomes) and microchannel resonators in MEMS with different properties according to similarity principle.

Our theoretical model can be used to quantify the natural frequencies and predict the changes (*e.g.*, monotonicity, mode appearance and disappearance) of the natural frequencies when the geometrical parameters (*e.g.*, slenderness ratio l/r_o and inner/outer radius ratio r_i/r_o) and mechanical parameters (*e.g.*, elastocapillarity number γ_{sl}/Er_o) are tuned. Since there are many liquid-filled capillary tubes that vibrate, our result can provide guidance in both the understanding of natural phenomena and design in engineering. On the one hand, the results can be used to rebuild structures to achieve certain natural frequencies such as the energy capture of capillary structures and improve the sensitivity of microchannel resonators by changing the structure; on the other hand, the results can be used to design structures to avoid resonance of certain frequencies such as precision instruments.

Declaration of competing interest

The authors declare that they have no known competing financial interests or personal relationships that could have appeared to influence the work reported in this paper.

CRediT authorship contribution statement

Shaobao Liu: Conceptualization, Methodology, Formal analysis, Writing - review & editing, Visualization. **Yufei Wu:** Methodology, Software, Formal analysis, Investigation, Writing - original draft, Writing - review & editing. **Fan Yang:** Software, Formal analysis, Validation. **Moxiao Li:** Formal analysis, Writing - review & editing. **Xing Kou:** Validation, Investigation. **Changsheng Lei:** Validation, Investigation. **Feng Xu:** Writing - review & editing, Supervision, Writing - review & editing, Funding acquisition. **Tian Jian Lu:** Writing - review & editing, Supervision, Resources, Project administration, Funding acquisition.

Acknowledgement

Appendix A. Supplementary data

Supplementary data to this article can be found online at https://doi.org/10.1016/j.mbbm.2020.103745.

References

Belardinelli, P., Ghatkesar, M., Staufer, U., Alijani, F., 2017. Linear and non-linear vibrations of fluid-filled hollow microcantilevers interacting with small particles. Int. J. Non Lin. Mech. 93, 30–40.

Bryan, A.K., Hecht, V.C., Shen, W., Payer, K.R., Manalis, S.R., 2013. Measuring single cell mass, volume, and density with dual suspended microchannel resonators. Lab Chip 14 (3), 569–576.

Burg, T.P., Manalis, S.R., 2003. Suspended microchannel resonators for biomolecule detection. Appl. Phys. Lett. 83 (13), 2698–2700.

Carrier, G.F., 1945. On the non-linear vibration problem of the elastic string. Q. Appl. Math. 3 (2), 157–165.

Gao, J., Kelly, R., Yang, Z., Chen, X., 2008. An investigation of capillary vibration during wire bonding process. In: International Conference on Electronic Packaging Technology & High Density Packaging, 2008. Icept-Hdp, pp. 1–6.

Girifalco, L.A., Good, R.J., 1957. A theory for the estimation of surface and interfacial energies. I. Derivation and application to interfacial tension. J. Phys. Chem. 61, 904–909.

Godin, M., Bryan, A.K., Burg, T.P., Babcock, K., Manalis, S.R., 2007. Measuring the mass, density, and size of particles and cells using a suspended microchannel resonator. Appl. Phys. Lett. 91 (12), 123121.

Gonçalves, P.B., Batista, R.C., 1988. Non-linear vibration analysis of fluid-filled cylindrical shells. J. Sound Vib. 127 (1), 133–143.

Good, R.J., Girifalco, L.A., 1960. A theory for the estimation of surface and interfacial energies. III. Estimation of surface energies of solids form contact angle data. J. Phys. Chem. 64, 561–565.

Hatfield, F.J., Wiggert, D.C., Otwell, R.S., 1982. Fluid structure interaction in piping by component synthesis. J. Fluid Eng. 104 (3), 318–325.

Hu, C.M., Guo, N.Q., Yu, J.D., Ling, S.F., 1999. The vibration characteristics of capillary in wire bonder. In: Electronics Packaging Technology Conference, 1998, pp. 202–205.

Keller, J.B., 1959. Large amplitude motion of a string. Am. J. Phys. 27 (8), 584–586.

Khan, M.F., Schmid, S., Larsen, P.E., Davis, Z.J., Yan, W., Stenby, E.H., Boisen, A., 2013. Online measurement of mass density and viscosity of pL fluid samples with suspended microchannel resonator. Sensor. Actuator. B Chem. 185, 456–461.

Kim, K.H., Bahl, G., Lee, W., Liu, J., Tomes, M., Fan, X., Carmon, T., 2012. Cavity optomechanics on a microfluidic resonator with water and viscous liquids. Physics 2 (11), e110.

Lee, I., Park, K., Lee, J., 2012. Note: precision viscosity measurement using suspended microchannel resonators. Rev. Sci. Iinstrum. 83 (11), 116106.

Liu, S., Jiao, J., Lu, T.J., Xu, F., Pickard, B.G., Genin, G.M., 2017. Arabidopsis leaf trichomes as acoustic antennae. Biophys. J. 113 (9), 2068–2076.

Marur, S.R., Prathap, G., 2005. Non-linear beam vibration problems and simplifications in finite element models. Comput. Mech. 35 (5), 352–360.

Najmzadeh, M., Haasl, S., Enoksson, P., 2007. A silicon straight tube fluid density sensor. J. Micromech. Microeng. 17 (8), 1657–1663.

Nandwana, B.P., Maiti, S.K., 1997. Modelling of vibration of beam in presence of inclined edge or internal crack for its possible detection based on frequency measurements. Eng. Fract. Mech. 58 (3), 193–205.

Sharma, P., Ganti, S., Bhate, N., 2003. Effect of surfaces on the size-dependent elastic state of nano-inhomogeneities. Appl. Phys. Lett. 82 (4), 535–537.

Timoshenko, S.P., 1983. History of Strength of Materials, with a Brief Account of the History of Theory of Elasticity and Theory of Structures. McGraw-Hill Book Company, Inc., New York-Toronto-London.

Ting, E.C., Hosseinipour, A., 1983. A numerical approach for flow-induced vibration of pipe structures. J. Sound Vib. 88 (3), 289–298.

Vargaftik, N., Volkov, B., Voljak, L., 1983. International tables of the surface tension of water. J. Phys. Chem. Ref. Data 12 (3), 817–820.

Wang, G.F., Feng, X.Q., 2007. Effects of surface stresses on contact problems at nanoscale. J. Appl. Phys. 101 (1), 013510.

Xia, R., Li, X., Qin, Q., Liu, J., Feng, X.Q., 2011. Surface effects on the mechanical properties of nanoporous materials. Nanotechnology 22 (26), 265714.

Zhou, L.H., Liu, S.B., Wang, P.F., Lu, T.J., Xu, F., Genin, G.M., Pickard, B.G., 2017. The Arabidopsis trichome is an active mechanosensory switch. Plant Cell Environ. 40 (5), 611–621.